Mass-Analyzed Threshold Ionization Spectra of $C_6H_6^+$ and $C_6D_6^+$ Obtained via the $^3B_{1u}$ Triplet State

Andrew B. Burrill, Jia T. Zhou, and Philip M. Johnson*

Department of Chemistry, State University of New York at Stony Brook, Stony Brook, New York 11794-3400

Received: December 6, 2002; In Final Form: April 15, 2003

The first mass-analyzed threshold ionization (MATI) spectra from molecular excited triplet states have been collected for benzene and perdeuteriobenzene from the $^3B_{1u}$, lowest triplet state. From these spectra, the C_6H_6 $^3B_{1u}$ state energy is found to be 29 627 ± 12 cm^{-1} and the C_6D_6 $^3B_{1u}$ state energy is found to be 29 828 ± 12 cm^{-1}. The MATI spectrum for each species was collected from 1000 cm^{-1} below the ionization threshold to ∼2000 cm^{-1} above the threshold. Hot band structure allowed for the first higher-resolution gas phase vibrational measurement of the ν_1, ν_8, and ν_6 frequencies in the $^3B_{1u}$ state. They were found at 927, 229, and 575 cm^{-1} for the protonated molecule and at 832, 200, and 528 cm^{-1} for the deuterated molecule, respectively. New vibrational structure has also been observed in the cation ground state of both molecules.

Introduction

The triplet manifold of benzene has been the subject of numerous investigations aimed at determining the ordering of the electronic states, the distortion in the geometries relative to the singlet state, and the intensities observed in spin-forbidden and orbitally forbidden transitions. A. C. Albrecht was the first to definitively identify the ordering of electronic states by explaining that the $^3B_{1u}$ state must be the lowest-energy state in the triplet manifold.[1] His work in defining the vibronic coupling mechanism through which the $^3B_{1u}$ state gains intensity has been referenced nearly 200 times, demonstrating the interest this work has had in the field of molecular spectroscopy. In this paper, we hope to contribute to the understanding of the spectroscopy of both the lowest triplet state of benzene and the ground state of the cation through the analysis of the mass-analyzed threshold ionization (MATI) spectra of benzene and perdeuteriobenzene, originating from the $^3B_{1u}$ state.

While the benzene triplet state serves as a model for states with strong vibronic coupling and weak spin−orbit coupling, because of the latter it has been very difficult to study experimentally. Direct absorption from the ground singlet state has never been observed for the pure gas. Phosphorescence gives information about the vibronic coupling in the state but not about its vibrational structure.[2] Phosphorescence excitation in crystals has provided triplet state vibrational structure, but at the expense of crystal field effects.[3] Electron energy loss spectra (both in the gas phase and from crystals) give some vibrational structure, but only at low resolution.[4−6] Oxygen-perturbed gas and crystal phase absorptions are both perturbed and low-resolution.[7−9]

Since attempts at triplet state spectroscopy from a lower electronic state have not proven to be definitive, an alternative approach would be to collect spectra from the triplet state to a higher electronic state. Triplet state information could be gleaned from the hot bands in the spectrum. As it turns out, the most conveniently used higher electronic state for obtaining highly resolved spectra is the ground state of the cation, and MATI spectroscopy provides a means of examining this transition. An adequate population of vibrationally warm triplet states is obtained by means of an electric discharge in a supersonic beam.

The $^3B_{1u}$ state is predicted to be highly distorted along the ν_8 ring stretching mode,[7] and has two configurations in which it may be confined in a crystal matrix. These geometries are described as quinoidal and antiquinoidal, where the carbon skeleton possesses two short and four long bonds and two long and four short bonds, respectively. The cause of this distortion is a pseudo-Jahn−Teller interaction with the nearby $^3E_{1u}$ state,[10] induced by the various e_{2g} vibrational modes (modes 6 to 9 in Wilson's notation). By obtaining the vibrational frequencies of the triplet state in the gas phase, one can obtain a more accurate understanding of the unconstrained potential energy surface of the triplet state.

MATI spectroscopy and its complementary technique, zero-electron kinetic energy (ZEKE) spectroscopy, have often been used to investigate the vibrational and rotational structure of the ground (D_0) state of the benzene cation.[11−23] The reason for this work has been, at least in part, its role as a prototypical Jahn−Teller (JT) active system. The understanding of this remarkable type of vibronic coupling relies on a thorough analysis of the complicated vibrational structure that arises from the JT effect. In particular, as much information as possible about the four e_{2g} JT active modes is desirable. To date, only one of these modes (6) has been adequately characterized. One of the reasons for the sole characterization of mode 6 is that all of these experiments have used a pump−probe excitation scheme where the ionization threshold is reached by two photons via a vibrational level (usually 6^1) of the lowest excited singlet state, S_1.

The JT effect is a form of vibronic coupling that can take place in any nonlinear molecule with degenerate electronic states. In the case of the benzene cation, the $^2E_{1g}$ electronic states may couple with the degenerate e_{2g} normal modes to produce a multitude of vibronic states and thoroughly mix the vibrational motions. By obtaining the experimental line positions for these e_{2g} normal modes, one can derive the JT coupling parameters, and consequently the shape of the molecular potential energy

* To whom correspondence should be addressed: Department of Chemistry, State University of New York at Stony Brook, Stony Brook, NY 11794-3400. E-mail: philip.johnson@sunysb.edu. Phone: (631) 632-7912.

10.1021/jp027643g CCC: $25.00
Published on Web 05/15/2003

surface. The reader desiring a more in-depth understanding of the JT effect is referred to one of the many review articles written on the subject,[24,25] or two recent papers focused exclusively on the JT effect in the benzene cation.[26,27]

It has been evident in several previous studies[28−31] of benzene and substituted benzene cations, using photoinduced Rydberg ionization (PIRI) spectroscopy,[31−33] that it is rarely possible to unambiguously understand the vibrational structure of a state using only a spectrum from a single lower state. There is not enough information in a single spectrum to resolve the multitude of possible assignments available in the dense vibrational manifolds of these states. In PIRI spectroscopy, the multiresonant nature of the process allows the recording of spectra from many lower states with different symmetries. However, this has not been possible for MATI or ZEKE spectroscopy of benzene through the S_1 state because of the dominant nature of the ν_6 vibrations in that state.

Because of the different electronic symmetry, MATI spectra from the lowest excited triplet states, $^3B_{1u}$, of benzene and perdeuteriobenzene have the potential for allowing additional vibrational structure to be seen in the cation. The fact that two of the JT active modes in the benzene cation, modes 8 and 9, appear very strongly in the phosphorescence spectrum indicates a good possibility of seeing these modes in the MATI spectra from the triplet state.

Experiment

The experimental apparatus used for these studies has been previously described and is only discussed here for clarity as well as to mention several new additions to the discharge and ionization design.[34,35] The experiment is carried out by combining the techniques used in prior MATI studies[36−41] and the discharge techniques used in several multiphoton ionization experiments performed in this laboratory.[34,35]

Because of the modest energy difference between the triplet state and the ionization threshold, the laser system needed for this set of experiments is greatly reduced from other benzene studies that required the use of either two or three independently pumped tunable dye lasers. In the experiments described here, only one Nd:YAG pump laser and one dye laser are needed. Additionally, there is no longer the added problem of having to overlap laser beams both temporally and spatially. However, the minimal sample density prevented the use of high-resolution MATI techniques.

A pulsed Quantel Nd:YAG laser operating at 10 Hz is used to pump a Quantel PDL-50 dye laser operating with either Coumarin 440 (430 nm − 450 nm), Coumarin 450 (440 nm − 480 nm), or Stilbene 420 (430 nm − 415 nm) dye. The dye laser output is doubled in a BBO crystal housed in an Inrad Autotracker III to generate the desired doubled photon wavelength. Scanning the dye laser and using the Autotracker III to continuously tune the doubling crystal then allows the complete MATI spectrum of the cation to be collected.

To generate an adequate number density of the long-lived triplet states needed for these experiments, a high-voltage electric discharge was used in conjunction with a pulsed supersonic expansion. This technique went through several iterations in an effort to obtain an experimental setup with the best stability and longevity. The choice of carrier gas turned out to be rather important for these experiments, and by experimenting with He, Ar, and N_2 carrier gases, we found that N_2 produces the best triplet state beam. The Ar carrier produced an adequate discharge, but a weaker signal. The discharge produced in the He carrier gas was very unstable, which negated its use.

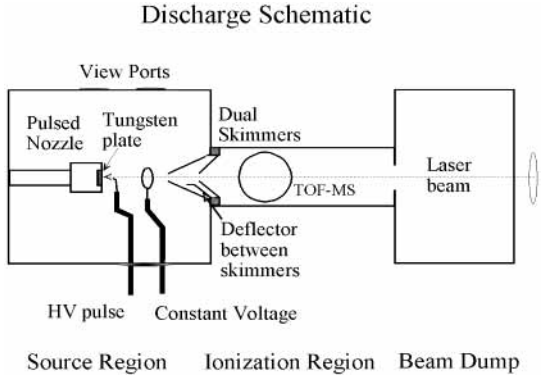

Figure 1. Discharge schematic employed in these experiments in which a high-voltage pulse is used and a continuous dc voltage on the ring is used to generate the triplet species.

The N_2 carrier gas, at a stagnation pressure of 2 bar, was passed over the room-temperature sample of benzene, causing the benzene vapor to become entrained in the N_2 carrier gas. The sample was then supersonically expanded through a General Valve pulsed nozzle operating at 10 Hz.

The triplet state benzene was generated via electric discharge in the expanding gas. Figure 1 shows the diagram of the electric discharge configuration in the chamber. The discharge was maintained between the nozzle and a tungsten ring, held at a constant voltage of 400−750 V (dc), located approximately 25 mm downstream from the nozzle face. A high-voltage 40 kV pulse from a sharpened tungsten rod, located 5 mm from the nozzle face, was used to initiate the discharge on each gas pulse.

Several unwanted side effects occur in an electric discharge, and care must be taken to minimize or eliminate these side effects. First, the discharge terminates on the nozzle, and the iron in the stainless steel there is ablated, resulting in a large number of Fe atomic lines appearing in the spectra. While this provides a very good source for wavelength calibration, it is otherwise a nuisance. The mass 56 Fe lies close enough to the benzene MATI signal that it can overwhelm the MATI peak if a strong atomic line lies at the same wavelength as one of the vibrations of the benzene cation.

To reduce the amount of Fe generated by the discharge, a tungsten disk was inserted into the nozzle face. A 1 mm diameter hole in the disk allowed the molecular beam to pass through but reduced the amount of Fe appearing in the spectra by providing an alternate ground for the discharge (some iron still appeared from further inside the nozzle). There is less ablation from tungsten than from iron, and what is ablated does not hinder the detection of the benzene MATI signal due to tungsten's significantly higher mass.

Another source of signal degradation was the creation of spurious ions from the discharge that made their way into the ionization region, and subsequently to the detector. To remove some of these spurious ions, two skimmers were placed in front of the sample entering the ionization region, and a deflector plate [450 V (dc)] was placed between them (see Figure 1). This helped to greatly reduce the background of ions that found their way to the detector when either no deflector voltage was applied or the two skimmers were not used.

In these experiments, the laser beam was introduced directly down the molecular beam instead of perpendicular to it (as in most of our previous work[37−41]). This was possible due to the fact that only a single laser was being used, and had the advantage of producing a much longer interaction region in

which the high-*n* Rydberg molecules could be generated. This resulted in a 4-fold increase in the magnitude of the MATI signal.

To further reduce spurious signals caused by ions produced by the electric discharge, a modified extraction scheme was used. This was accomplished by holding the repeller at a high voltage, 725 V/cm, until just prior to the intersection of the laser beam with the molecular beam, when it was changed to 0 V/cm to allow the Rydberg molecules to be formed in zero field. After the laser beam intersected the molecular beam, a separation voltage of 2−4 V/cm was applied for approximately 3 μs to move the directly produced ions away from the high-*n* Rydberg molecules. Following this separation, the repeller was returned to its initial voltage of 725 V/cm field, ionizing the high-*n* Rydberg molecules and sending them and the directly produced ions up the flight tube as in a standard MATI experiment. Holding the high voltage on the plates until just before the laser fired provided fringe fields that helped prevent the ions generated in the discharge from entering the ionization region along the path of the molecular beam.

After the ions traveled up the flight tube, the ion signal was collected by a set of 40 mm multichannel plates (MCP) interfaced with a transient digitizer and personal computer. The mass spectrum was then collected at every laser shot and averaged for typically 100 or 120 shots before the instrument stepped to the next wavelength.

Discharge Mechanism

The mechanism for the creation of triplet states in a seeded discharge is undoubtedly complex. Different possibilities for benzene excitation include direct electron impact promotion into either the singlet or triplet manifolds, electron−ion recombination, and energy transfer from excited electronic states of the carrier gas. The fact that the nitrogen carrier is superior in producing the benzene triplet lends credence to the latter mechanism being important. It is well-known that a discharge in N_2 produces a variety of fairly low-lying metastable excited states, both singlet and triplet. The lowest triplet of N_2, the A $^3\Sigma_u^+$ state, has a lifetime of seconds and an energy of only ~6 eV, for example. The B, a, and a′ levels also have long lifetimes and could participate in energy transfer without depositing undue amounts of energy into the benzene. Alternatively, the C to B transition energy (the second positive system, active in N_2 lasers) is nearly isoenergetic to benzene's triplet state and could provide a means of resonance energy transfer. On the other hand, the lowest excited state of argon is at 11.5 eV and energy transfer from that atom may produce more fragmentation and ionization than parent excitation.

If excess energy is deposited into the molecule, an electronic and vibrational cascade process must then follow. This has to take place in the collisional region at the exit of the nozzle, before the supersonic expansion has taken away the relative kinetic energy of the gas. Any states that enter into the collisionless beam must live for several hundred microseconds to reach the ionization region of the apparatus. This puts a lower limit of 375 μs on the lifetimes of vibrational levels in the triplet state up to the energy of the ν_1 vibration at 927 cm^{-1}. Transitions from higher-energy vibrational levels are not seen in the MATI spectra, because either the state lifetimes are too short or the oscillator strengths are too small.

Spectral Analysis

The MATI spectra of $C_6H_6^+$ and $C_6D_6^+$ are shown in Figures 2 and 3, respectively, with the line positions listed in Table 1.

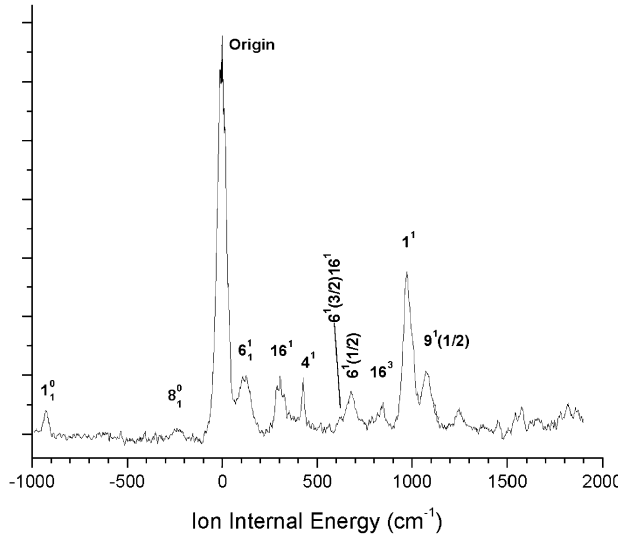

Figure 2. MATI spectrum of $C_6H_6^+$ from the triplet state with the vibrational assignments given in Table 1.

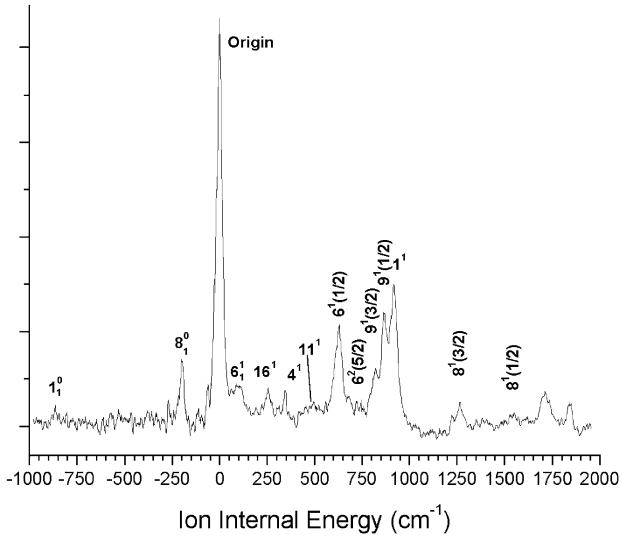

Figure 3. MATI spectrum of $C_6D_6^+$ from the triplet state with the vibrational assignments listed in Table 1.

The lowest triplet state energy, $^3B_{1u}$, can be obtained from the MATI spectrum by subtracting the ionization photon wavelength from the known ionization potential. The ionization potentials obtained by Neuhauser et al.[19] from high-resolution Rydberg excitation experiments were used for this purpose. The $C_6H_6^+$ ionization potential lies at 74 556 cm^{-1} and is reached from the triplet using a 222.54 nm, or 44 935 cm^{-1}, photon. This provides a value for the triplet state energy of 29 627 ± 12 cm^{-1}. This energy has been corrected for the depression in the Rydberg manifold ($D = 4\sqrt{F}$) caused by the MATI separation element, *F*, of 2.5 V/cm.[42]

The triplet energy presented here is in good agreement with the most recent previous experimental gas phase triplet state energy of 29 639 cm^{-1} (3.674 eV), obtained by Sharpe and Johnson in 1984 by measuring the total ion threshold.[34] The total ion thresholds are so abrupt for these transitions that little error was introduced in using the less precise technique. The triplet energy also agrees with three recent theoretical papers that calculated the energy levels for the triplet states of benzene using high-level *ab initio* CASSCF or coupled cluster response theory methods.[43−45] In the *ab initio* calculations, the triplet state

TABLE 1: Vibrational Assignments from the Single-Photon MATI Spectrum Obtained via the T_1 Triplet State of both C_6H_6 and C_6D_6

vibrational assignment	$C_6H_6^+$	$C_6D_6^+$	vibrational assignment	$C_6H_6^+$	$C_6D_6^+$
1^0_1	−927	−832	$9^1(3/2)$		822
		−274	9^1	1071	863
8^0_1	−229	−200	1^1	972	916
16^1_1		−111	$6^2(3/2)$	1247	
16^1_1		−63	$8^1(3/2)$		1224
origin	0	0	$8^1(3/2)$	1373	1263
6^1_1	120	101			1320
16^1	285	220		1450	1354
16^1	303	255		1505	
16^1	330			1542	1408
$6^1(3/2)$	353			1577	
4^1	423	345		1629	
11^1		496		1661	1550
16^2		560			1619
$6^1(3/2)16^1$	622			1782	1711
$6^1(1/2)$	675	629		1821	1733
$6^2(5/2)$		682			1797
$6^2(5/2)$		722		1861	1839
16^3	846				

energy was found to be 3.962 eV[43] (31 955 cm^{-1}), 4.349 eV[44] (35 074 cm^{-1}), and 3.83 eV[45] (31 052 cm^{-1}).

The MATI spectrum of $C_6H_6^+$ covers a range from 1000 cm^{-1} below the IP to 1900 cm^{-1} above the IP. Two significant hot band peaks appear below the IP. They are the 8^0_1 hot band at −229 cm^{-1} and 1^0_1 hot band at −927 cm^{-1}. These transitions provide accurate vibrational frequencies for both of these modes in the $^3B_{1u}$ gas phase, and they can also be used to identify additional vibrational structure that may contain either of them. No significant ion signal is present below the 1^0_1 transition, due to either the lifetime of the triplet state or the lack of oscillator strength, as previously mentioned.

The appearance of the 8^0_1 hot band in the gas phase MATI spectrum is of interest since the ν_8 frequency in the triplet state (229 cm^{-1}) is significantly lower than in S_0 and S_1 (∼1500 and ∼1600 cm^{-1}, respectively) and has been the subject of many papers over the past 40 years.[1,3,7,9,46−51] The interest in ν_8 in the $^3B_{1u}$ state lies in the fact that the $^3B_{1u}$ state is pseudo-JT active, and must vibronically couple to the $^3E_{1u}$ state to gain any oscillator strength in phosphorescence. This coupling can only occur through the four e_{2g} modes, and it has been shown that the ν_8 stretching mode is the most likely vibration to induce this coupling.[28,47] The strong appearance of ν_8 in the triplet MATI hot band spectrum emphasizes the strong vibronic interaction of that mode in the cation ground state. The Jahn−Teller effect mixes ν_8 strongly into the zero vibrational level in the $^2E_{1g}$ state, producing good vibrational overlap with the ν_8 vibration of the triplet. It does not appear as strongly in the cation vibrational structure because the Jahn−Teller mixing dilutes its oscillator strength and it is not as strongly mixed into the origin in the triplet state.

In the $^3B_{1u}$ state, the potential energy minimum of the molecule is displaced considerably from the ground state configuration due to the fact that an electron has been promoted to an antibonding orbital, and the aromatic structure of the ring has been lost. Buma et al.[47] calculated the potential energy surface along the ν_8 coordinate and showed that it is a very flat and wide potential from the pseudo-JT interaction. The significantly lower frequency of the ν_8 normal mode in the $^3B_{1u}$ state is thus attributed to the shape of the potential energy surface.

The MATI value for ν_8 in the triplet state is somewhat lower than the previously reported experimental values of Burland et al.[3] and King and Pinnington.[7] The latter report an oxygen-perturbed gas phase value of ∼250 cm^{-1}, while Burland et al. observe two peaks in a crystal matrix at 239 and 252 cm^{-1} that they attribute to splitting due to the pseudo-JT effect. No splitting is observed in our spectrum, nor has it been reported in any of the other gas phase spectra. Furthermore, Buma et al.[47] indicate that there should be no splitting due to the pseudo-JT activity but that it can be induced by crystal field effects.

Immediately above the origin, at 107 cm^{-1}, there is a hot band of considerable intensity. The most likely assignment for a transition that would possess this much intensity is the 6^1_1 transition from ν_6 in the triplet state to the 6(1/2) JT component of ν_6 in the cation. This observation yields a gas phase ν_6 frequency in the triplet state of 575 cm^{-1}, a change of approximately 50 cm^{-1} relative to the frequency in the crystal.[3] A deviation in frequency from the value obtained in the crystal is plausible due to the effects the matrix has on the molecule, and is a change proportionally similar to ν_8.

The next set of peaks at 285, 303, and 330 cm^{-1} are those making up the ν_{16} vibration, split by the quadratic JT coupling. A small peak at 353 cm^{-1} is identified as one of the $6^1(3/2)$ peaks, while the 4^1 normal mode is found at 423 cm^{-1}. The next strong peak appearing in the spectrum is the $6^1(1/2)$ peak at 675 cm^{-1}, with a small shoulder to the low-energy side that is tentatively assigned as the $6^1(3/2)16^1$ combination band. With a move to a higher energy, another group of peaks is found centered at 845 cm^{-1}, assigned as the 16^3 overtone.

The most intense peak found in the spectrum appears at 972 cm^{-1}, and is the totally symmetric ring breathing mode, ν_1. A very interesting feature appears in the spectrum at 1071 cm^{-1}, and is assigned as the $9^1(1/2)$ normal mode, with the $9^1(3/2)$ component appearing as a weak shoulder on the high-energy side of ν_1. The appearance of this JT active mode is fortuitous, and will be useful in the determination of the cation JT fitting parameters in future work.

The remainder of the $C_6H_6^+$ MATI spectrum cannot be assigned without full JT calculations and reference to MATI spectra from other states. This analysis is in progress, and the complete analysis of the JT effect will be presented in a future paper.

A theoretical analysis of the JT effect in benzene cation[26] has led to the conclusion that the JT modes in the benzene cation are very well mixed in all the lower degenerate states. Experiment has shown this prediction to be born out for the B state of the benzene cation,[27] and it is expected to be the case for the ground state also. In particular, modes 6, 8, and 9 have such large JT couplings that by the time the energy of ν_8 is reached, it is almost misleading to speak of "assignments". However, the comparison of relative intensities in different spectra may indicate transitions that have identifiable character, and thus enable JT calculations to proceed with more confidence.

Significantly, it is possible that two peaks with a significant contribution from ν_8 appear (at 1373 and 1661 cm^{-1}) weakly in this spectrum. The intensity in these bands may be lacking because the extensive JT mixing in the cation has diluted the oscillator strength of ν_8. It is also possible that the Franck−Condon overlap for ν_8 in the transition from the triplet state to the cation is poor because of the enormous change in the character of the mode.

The $C_6D_6^+$ MATI spectrum, shown in Figure 3, has an ionization potential of 74 583 cm^{-1} reached using a 223.41 nm, or 44 760 cm^{-1}, photon. This results in the triplet state being located at 29 828 ± 12 cm^{-1}, again accounting for the MATI separation element (F = 2 V/cm). This value is also in good

agreement with the previous total ion threshold measurement that lists the triplet state energy as 29 837 cm^{-1}.[34]

The normal mode assignment of the $C_6D_6^+$ MATI spectrum follows very closely that of the $C_6H_6^+$ MATI spectrum. The hot band structures corresponding to the 1^0_1 and 8^0_1 peaks are found at −832 and −200 cm^{-1}, respectively, with the 6^1_1 hot band at 103 cm^{-1}. This ν_6 hot band again provides the $^3B_{1u}$ ν_6 frequency of 528 cm^{-1} in the gas phase.

In this spectrum, the ν_{16} normal mode is seen as a single broad peak at 255 cm^{-1} with a small unassigned peak found at 310 cm^{-1}. The 4^1 peak at 345 cm^{-1} falls directly over the location of the $6^1(3/2)$ peaks, and therefore, they do not appear in this spectrum. Two peaks found in the deuterated spectrum but not the protonated one appear at 496 and 560 cm^{-1} and are assigned as the 11^1 and 16^2 normal modes, respectively. The $6^1(1/2)$ peak appears significantly stronger than in the protonated spectrum and lies at 629 cm^{-1}, with two small peaks tentatively assigned as $6^2(5/2)$ found slightly higher in energy at 682 and 722 cm^{-1}. It should be noted that all the assignments of the small features in the spectra benefit from comparison of these spectra to other MATI spectra of the cation ground state from the neutral ground state and from S_1.

This again leads to an interesting region of the spectrum. The ν_9 JT active mode is present in the deuterated spectrum with considerably more intensity than in the protonated spectrum. It is possible to make out both the $9^1(3/2)$ and $9^1(1/2)$ angular momentum components at 822 and 863 cm^{-1}, respectively. With this information, it will be possible to calculate the linear coupling term for ν_9 along with the effect it may have when mixed with other JT active modes. The reason for the increased intensity of ν_9 in the deuterated spectrum compared to the protonated spectrum rests in the effect the mass of the deuterium has on the ν_9 normal mode relative to the mass of hydrogen.

This "deuterium effect" has been discussed by Johnson and Ziegler[52] in their phosphorescence study of C_6H_6 and C_6D_6. In C_6H_6, the ν_9 normal mode is made up of an in plane hydrogen wag, where there is little or no oscillation of the carbon−carbon bond lengths in the protonated molecule. However, upon deuterium substitution, the carbon−carbon bond lengths are perturbed by the motion of the deuterium atoms, the effective increase in mass having affected the motion of the carbon atoms. It was concluded that the difference in the intensity of ν_9 in the phosphorescence of the isotopomers is related to the fact that the oscillator strength, induced by the vibronic coupling, is increased in the deuterated molecule relative to that in the protonated molecule.

Returning to the identification of the remainder of the $C_6D_6^+$ spectrum, we find the ν_1 peak at 916 cm^{-1} followed by peaks at 1224, 1263, and 1550 cm^{-1} that may contain substantial ν_8 character. Definitive assignment of these peaks may be possible once further analysis is completed.

The widths of the peaks in these MATI spectra are larger than the MATI spectra typically obtained in our laboratory. One of the reasons for this lies in the fact that for most of our previously published spectra a "high-resolution" MATI technique was employed. This was accomplished by using either a small step voltage to separate the Rydbergs from the prompt ions[38] or two separation elements, a small negative voltage, followed by an equivalent positive voltage,[53] to obtain a smaller distribution of high-*n* Rydberg molecules prior to field ionization. The resolution obtained using those techniques is typically on the order of ±4 cm^{-1} or better (usually determined by the width of the rotational envelope), but is obtained at the cost of the intensity of the MATI signal. For our pump−probe and VUV MATI spectra, the signal has been sufficiently strong to accept this loss in exchange for the higher resolution. However, such was not the case for the experiments carried out here, and the high-resolution techniques could not be used.

The second cause of the line broadening can be the use of the high-voltage electric discharge used to generate the triplet states. The electric discharge creates a rotationally and vibrationally warm beam that leads to broader line shapes. Additionally, the use of N_2 as the carrier gas does not rotationally cool the benzene as well as the use of inert gases.

Conclusion

This paper has presented the first MATI spectrum of the benzene cation originating from the lowest excited triplet state, $^3B_{1u}$. Several new features have been found in both the $^3B_{1u}$ and $^2E_{1g}$ states of benzene and perdeuteriobenzene. The $^3B_{1u}$ energy level has been more precisely measured for both $C_6H_6^+$ and $C_6D_6^+$ using the threshold ionization technique in conjunction with the known values of the ionization potentials of these molecules. Additionally, high-quality gas phase experimental frequencies were obtained for the ν_1, ν_6, and ν_8 normal modes in the triplet state.

Significant progress has been made in obtaining experimental values for the JT active modes in the ground state of the cation. Vibrations with substantial ν_8 and ν_9 character have been tentatively identified in the triplet MATI spectra presented here, and the experimental line positions will be used for comparison with the MATI spectra collected using other excitation schemes.

Finally, since the HV electric discharge created a very warm molecular beam, and the resolution obtained in these spectra is not as good as that obtained using the high-resolution MATI technique, future work with the triplet state may involve generating the $^3B_{1u}$ state using laser excitation. By exciting single rotational lines, one can form a much colder rotational distribution. Additionally, the high-resolution MATI technique may then be applicable, and the line positions obtained here can be refined. The other advantage of using laser excitation lies in reducing the background of Fe^+ and N_2^+ found in these spectra, which again aided in the identification of some of the weaker benzene normal modes.

In summation, several high-resolution vibrational assignments in both the $^3B_{1u}$ and $^2E_{1g}$ state have been made. These data should aid the theoretical efforts that have been put forth to further the understanding of the structure of both the cation and the triplet state.

Acknowledgment. This work was supported by the U.S. Department of Energy, Basic Energy Sciences, through Grant FG02-86ER13590.

References and Notes

(1) Albrecht, A. C. *J. Chem. Phys*. **1963**, *38*, 354−365.
(2) Johnson, P. M.; Ziegler, L. *J. Chem. Phys.* **1972**, *56*, 2169−2175.
(3) Burland, D. M.; Castro, G.; Robinson, G. W. *J. Chem. Phys*. **1970**, *52*, 4100−4108.
(4) Swiderek, P.; Schurfeld, S.; Winterling, H. *J. Phys. Chem*. **1997**, *101*, 1517−1526.
(5) Swiderek, P.; Michaud, M.; Sanche, L. *J. Chem. Phys*. **1996**, *105*, 6724−6732.
(6) Wilden, D. G.; Comer, J. *J. Phys. B: At., Mol. Opt. Phys.* **1980**, *13*, 627−640.
(7) King, G. W.; Pinnington, E. H. *J. Mol. Spectrosc*. **1965**, *15*, 394−404.
(8) Colson, S. D.; Bernstein, E. R. *J. Chem. Phys.* **1965**, *43*, 2661−2668.
(9) Metcalfe, J.; Rockley, M. G.; Phillips, D. *J. Chem. Soc., Faraday Trans. 2* **1974**, *70*, 1660−1666.

(10) van der Waals, J. H.; Berghuis, A. M. D.; de Groot, M. S. *Mol. Phys*. **1967**, *13*, 301−321.
(11) Müller-Dethlefs, K.; Sander, M.; Chewter, L. A. *Laser Spectroscopy VII: Proceedings of the Seventh International Conference*, Honolulu, HI, June 24−28, 1985; Hänsch, T. W., Shen, Y. R., Eds.; Springer-Verlag: Berlin, 1985; pp 118−121.
(12) Chewter, L. A.; Sander, M.; Müller-Dethlefs, K.; Schlag, E. W. *J. Chem. Phys*. **1987**, *86*, 4737−4744.
(13) Lindner, R.; Sekiya, H.; Beyl, B.; Müller-Dethlefs, K. *Angew. Chem., Int. Ed. Engl*. **1993**, *32*, 603−606.
(14) Lindner, R.; Sekiya, H.; Müller-Dethlefs, K. *Angew. Chem., Int. Ed. Engl*. **1993**, *32*, 1364−1366.
(15) Sekiya, H.; Lindner, R.; Müller-Dethlefs, K. *Chem. Lett*. **1993**, *3*, 485−488.
(16) Krause, H.; Neusser, H. J. *J. Chem. Phys*. **1993**, *99*, 6278−6286.
(17) Smith, J. M.; Zhang, X.; Knee, J. L. *J. Phys. Chem*. **1995**, *99*, 1768−1775.
(18) Neuhauser, R.; Neusser, H. J. *Chem. Phys. Lett*. **1996**, *253*, 151−157.
(19) Neuhauser, R. G.; Siglow, K.; Neusser, H. J. *J. Chem. Phys*. **1997**, *106*, 896−907.
(20) Held, A.; Baranov, L. Y.; Selzle, H. L.; Schlag, E. W. *J. Chem. Phys*. **1997**, *106*, 6848−6862.
(21) Siglow, K.; Neusser, H. J. *J. Chem. Phys*. **2000**, *112*, 647−653.
(22) Siglow, K.; Neusser, H. J. *J. Electron Spectrosc*. **2000**, *112*, 199−207.
(23) Bakker, J. M.; Satink, R. G.; von Helden, G.; Meijer, G. *Phys. Chem. Chem. Phys*. **2002**, *4*, 24−33.
(24) Longuet-Higgens, H. C. *Adv. Spectrosc*. **1961**, *2*, 429−472.
(25) Barckholtz, T.; Miller, T. *Int. Rev. Phys. Chem*. **1998**, *17*, 435−524.
(26) Johnson, P. M. *J. Chem. Phys*. **2002**, *117*, 9991−10000.
(27) Johnson, P. M. *J. Chem. Phys*. **2002**, *117*, 10001−10007.
(28) Goode, J. G.; Hofstein, J. D.; Johnson, P. M. *J. Chem. Phys*. **1997**, *107*, 1703−1716.
(29) Goode, J. G.; LeClaire, J. E.; Johnson, P. M. *Int. J. Mass Spectrom*. **1996**, *159*, 49−64.
(30) Taylor, D. P.; Goode, J. G.; Johnson, P. M. *J. Chem. Phys*. **1995**, *103*, 6293−6295.
(31) Johnson, P. M.; Anand, R.; Hofstein, J. D.; LeClaire, J. E. *J. Electron Spectrosc*. **2000**, *108*, 177−187.
(32) Anand, R.; Hofstein, J. D.; Johnson, P. M. *J. Phys. Chem. A* **1999**, *103*, 8927−8934.
(33) Anand, R.; LeClaire, J. E.; Johnson, P. M. *J. Phys. Chem. A* **1999**, *103*, 2618−2623.
(34) Sharpe, S.; Johnson, P. *J. Chem. Phys*. **1984**, *81*, 4176−4177.
(35) Sharpe, S.; Johnson, P. *Chem. Phys. Lett*. **1984**, *107*, 35−38.
(36) Zhu, L.; Johnson, P. M. *J. Chem. Phys*. **1991**, *94*, 5769−5771.
(37) Hofstein, J. D.; Goode, J. G.; Johnson, P. M. *Chem. Phys. Lett*. **1999**, *301*, 121−130.
(38) Johnson, P. M.; Zhu, L. *Int. J. Mass Spectrosc*. **1994**, *131*, 193−209.
(39) Burrill, A. B.; Johnson, P. M. *Chem. Phys. Lett*. **2001**, *350*, 473−478.
(40) Burrill, A. B.; Johnson, P. M. *J. Chem. Phys*. **2001**, *115*, 133−138.
(41) Hofstein, J. D.; Johnson, P. M. *Chem. Phys. Lett*. **2000**, *316*, 229−237.
(42) Chupka, W. A. *J. Chem. Phys*. **1993**, *98*, 4520−4530.
(43) Hald, K.; Hattig, C.; Jorgensen, P. *J. Chem. Phys*. **2000**, *113*, 7765−7772.
(44) Hattig, C.; Kohn, A.; Hald, K. *J. Chem. Phys*. **2002**, *116*, 5401−5410.
(45) Hashimoto, T.; Nakano, H.; Hirao, K. *J. Chem. Phys*. **1996**, *104*, 6244−6258.
(46) Buma, W. J.; van der Waals, J. H.; van Hemert, M. C. *J. Am. Chem. Soc*. **1989**, *111*, 86−87.
(47) Buma, W. J.; van der Waals, J. H.; van Hemert, M. C. *J. Chem. Phys*. **1990**, *93*, 3733−3745.
(48) Ohno, K.; Takahashi, R. *Chem. Phys. Lett*. **2002**, *356*, 409−422.
(49) Osamura, Y. *Chem. Phys. Lett*. **1988**, *145*, 541−544.
(50) van der Waals, J. H.; Berghuis, A. M. D.; de Groot, M. S. *Mol. Phys*. **1971**, *21*, 497−521.
(51) van Egmond, J.; van der Waals, J. H. *Mol. Phys*. **1967**, *28*, 457−467.
(52) Johnson, P. M.; Ziegler, L. *J. Chem. Phys*. **1972**, *56*, 2169−2175.
(53) Dessent, C.; Haines, S.; Muller-Dethlefs, K. *Chem. Phys. Lett*. **1999**, *315*, 103−108.